Decentralized Voltage Control of Autonomous DC Microgrids With Robust Performance Approach

Derakhshan, Siamak; Shafiee-Rad, Marjan; Shafiee, Qobad; Jahed-Motlagh, Mohammad Reza; Sahoo, Subham; Blaabjerg, Frede

Published in:
I E E E Journal of Emerging and Selected Topics in Power Electronics

DOI (link to publication from Publisher):
10.1109/JESTPE.2021.3054723

Publication date:
2021

Document Version
Accepted author manuscript, peer reviewed version

This article has been accepted for publication in a future issue of this journal, but has not been fully edited. Content may change prior to final publication. Citation information: DOI 10.1109/JESTPE.2021.3054723, IEEE Journal of Emerging and Selected Topics in Power Electronics

Decentralized Voltage Control of Autonomous DC Microgrids with Robust Performance Approach

Siamak Derakhshan, Marjan Shafiee-Rad, Qobad Shafiee, *Senior Member, IEEE,* Mohammad Reza Jahed-Motlagh Subham Sahoo, *Member, IEEE,* and Frede Blaabjerg, *Fellow, IEEE*

***Abstract*—In this paper, we propose an optimal decentralized robust H_∞ control system for the voltage control problem of autonomous uncertain DC microgrids consisting of multiple Distributed Generations (DGs) with general topology. The one Degree of Freedom (DoF) structure of the developed control system guarantees the robust performance of the system as well as its robust stability against various sources of uncertainty such as Plug-and-Play (PnP) operation of the DGs, topology changes, large load perturbations, different subsequent system changes, and the presence of Constant Power Loads (CPLs). To that end, the uncertain DC microgrid is modeled as an LTI polytopic state-space system. Then, a state-feedback control technique based on Linear Matrix Inequality (LMI) with Linearly Parameter-Dependant (LPD) Lyapunov matrices is implemented on the uncertain DC microgrids. The proposed controller does not require any sort of communications, and the robust performance property of the controller eliminates the need for pre-filter design. The efficiency of the proposed controller is analyzed by simulating different case studies through SimPowerSystems Toolbox in Matlab. Finally, the performance of the proposed control method is validated via experimental studies.**

***Index Terms*—DC microgrids, linear matrix inequality (LMI), robust H_∞ control, robust performance, voltage control.**

NOMENCLATURE

Indices

i, j	Indices for DG units
ij	Index for distribution lines
v	Vertex number of polytopic uncertainty region

DG Parameters

d_{buck_i}	Duty cycle of buck converter of DG i
d_{boost_i}	Duty cycle of boost converter of DG i
C_{t_i}	Shunt capacitor of DG i
R_{t_i}, L_{t_i}	Series filter resistance and inductance of DG i
R_{ij}, L_{ij}	Distribution line resistance and inductance
Z_{ij}	Distribution line impedance
P_{CPL_i}	Constant power of the CPL in DG i
P_i	Output active power of DG i
V_i	PCC voltage of DG i
V_{t_i}	Converter terminal voltage of DG i
I_{t_i}	RL series filter current of DG i
I_{L_i}	Load current of DG i
I_{ij}	Distribution line current
V_{ref_i}	Voltage reference value of DG i
V_{dc_i}	DC bus voltage of DG i
f_{sw}	Switching frequency
f_0	System nominal frequency
f_s	Sampling frequency

Control Variables

W_i^v	Lyapunov matrix for vertex v of uncertainty in local controller of DG i
X_i, Z_i	Slack matrices in local controller of DG i
N_i	A subset containing the indices of the neighboring units of DG i
$N_{i_{max}}$	Maximum possible connections between DG i and other DGs
z_i	Controlled-output vector
η_i	Positive scalar variable
ϵ_i	Non-zero scalar variable
ζ_i	Scalar variable belong to $(-1, 1)$ interval
$\sqrt{\gamma}$	Upper bound for controlled-output to disturbance H_∞ norm
K_i	State-feedback gain vector

S. Derakhshan, M. Shafiee-Rad, and M. R. Jahed-Motlagh are with the Department of Electrical Engineering, Iran University of Science and Technology, Tehran, Iran, Emails: (siamak_derakhshan@elec.iust.ac.ir, shafiee_m@elec.iust.ac.ir, and jahedmr@iust.ac.ir).

Q. Shafiee is with the Department of Electrical Engineering, University of Kurdistan, Sanandaj, Kurdistan, Iran, Email: (q.shafiee@uok.ac.ir).

S. Sahoo and F. Blaadjerg are with the Department of Energy Technology, Aalborg University, Aalborg East, 9220, Denmark, Email: (sssa@et.aau.dk and fbl@et.aau.dk).

I. INTRODUCTION

In the past years, due to the DC characteristics of most renewable energy resources like photovoltaic and fuel cells along with energy storage sources, attitudes toward DC microgrids have been escalating [1]. In terms of load, many loads, such as electric vehicles and most motor drives, need DC power. Therefore, DC microgrids do not require multiple AC to DC and DC to AC converters. Generally, higher efficiency, lower price, greater reliability, and more power transmission capacity are the prominent features of this type of microgrids compared to the AC microgrids [2]-[4].

Due to the recent advances in power electronic converters, as well as the growing trend of using renewable energy resources, the design of a control system that can guaranty the stability and optimal performance of the DC microgrids has become highly crucial. The general approach for the control of microgrids is based upon a hierarchical control strategy, consisted of three control layers: primary, secondary, and tertiary. Fast voltage regulation and accurate power distribution among DGs are the responsibility of the controllers inside the primary control level. Secondary level corrects the voltage steady-state deviations that might have happened at

the primary level. Tertiary control, which has the highest level of control in hierarchical control, is accountable for designating the optimal set-points according to the conditions and requirements of the main grid [5].

Droop control method has been one of the main techniques for controlling the voltage of the islanded DC microgrids at the primary level of hierarchical control [6]-[14]. The basis of the droop-based methods for the DC microgrids is in the linear decrement of the voltage reference value by increasing the output current. In DC microgrids, the output current or power can be used as the feedback signal [7]. However, droop control methods have several drawbacks. For example, droop-based methods are not robust against load changes and non-linear or unbalanced loads, which can result in instability. These methods also create a compromise between the accuracy of current distribution and voltage regulation. Increasing the droop coefficients increases the accuracy of current distribution and also increases the damping of the system, but on the other hand, it causes voltage deviation, which again raises the need to use a secondary controller. Slow transient response, poor performance against resistive-inductive lines, voltage steady-state error and inability to attain a coordinated performance of multiple components with different characteristics are the main drawbacks of droop-based control methods [8]-[11].

Disadvantages of the droop-based control techniques have led the research into the non-droop control methods. In these methods, an advanced control system based upon the exact model of the microgrid is designed to achieve the stability and desirable performance of the overall microgrid system. Using a fully decentralized control strategy in non-droop-based control methods, the voltage control is achieved only using local measurements [15]. Therefore, the need for communication channels and problems such as delay, communication link failure, and etc., that arise in control methods based on non-decentralized control strategies would be eliminated. Given that one of the most significant challenges in the control of islanded microgrid systems is to insure their stability and desired performance against various sources of uncertainty, including PnP functionality of DGs, load variations, and topological changes, the robust control method has become the main approach among the non-droop based controllers.

While robust non-droop-based controllers are mostly implemented on AC microgrids [16]-[21], some researchers have implemented the non-droop control technique on DC microgrids as well, e.g. [22]-[27].

The majority of the robust control systems designed so far, provide robust stability of the islanded microgrid against loads variations, while failed to address the PnP functionality of DGs, topology changes, and robustness against the presence of CPLs [22]-[24]. Furthermore, robust performance of the system and generality of the topology of DC microgrid is neglected in most of the designed control systems [22]-[27]. For example, robustness against load variations was investigated in [22] and [23] through sub-optimal robust controllers. Also, robustness of the controller against the presence and uncertainty of CPLs and local ohmic loads were investigated in [24] through a sub-optimal three DoF robust controller. However, non-robustness against PnP operation of the DGs and microgrid topological variations, inability to provide robust performance, limited load modeling, and high complexity were the main drawbacks of the developed controllers in [22]-[24]. The problem of PnP operation of DGs is investigated through non-droop-based three DoF robust controllers in [25], [26] and [27]. First, authors in [25] presented a state-feedback robust controller that allowed PnP operation and provided robustness against load changes. However, controller parameters had to be re-tuned every time a DG plugged-in or out of the system. Afterward, another control approach for the PnP functionality of the DGs was proposed in [26]. Differently from [25], by proposing a line-independent modeling procedure, controller in [26] did not require any update in controller parameters after the PnP operation. Later, the authors in [27] designed a three DoF robust control system providing robust stability against the PnP operation, topology changes, and load changes without a need for any parameter re-tuning. All the designed controllers in [25]-[27], only stabilized the system while neglected the system's robust performance in the control design process that resulted in the system's poor performance against the PnP functionality of DGs and topological changes, and had a very complex design due their three DoF structure. Furthermore, due to using three independent optimization problems for the design of three DoF controllers, these approaches result in a sub-optimal design and non-robustness against several different subsequent changes. Also, the designed controllers in [25] and [26] did not provide robustness against the presence of CPLs. Multiple researches have been conducted on the extension of robust non-droop-based control method for DC microgrids; however, they comprise one or more of the following disadvantages, 1) non-robustness against PnP functionality of DGs [22]-[24], 2) inability to maintain robust performance under PnP functionality of DGs and topological changes [24]-[27], 3) sub-optimal controllers [22]-[27], 4) limitations to the Lyapunov matrices in the controller design process [24]-[27], 5) non-robustness to several different subsequent changes [24]-[27], 6) the need to design pre-filters and thus the complexity of the controller [24]-[27], 7) being inapplicable to DC microgrids with general topology [22], [23], and 8) non-robustness against the presence of CPLs [22], [23], [25], and [26].

The focus of this paper is to present a new optimal one DoF robust H_∞ control system for the voltage control problem of islanded multi-DG DC microgrid with a general topology. The main contributions of the proposed controller contrary to the previous works are:

- Unlike the controllers that have been designed so far, the proposed control system not only provides robust stability, but it also provides robust desired performance of the DC microgrid system under multiple sources of uncertainty such as PnP operation of DGs, microgrid topology changes, load variations, different subsequent system changes, and presence of the CPLs.
- Opposed to what was presented in [23]-[27], the proposed one DoF control system is the solution of a unique convex

This article has been accepted for publication in a future issue of this journal, but has not been fully edited. Content may change prior to final publication. Citation information: DOI 10.1109/JESTPE.2021.3054723, IEEE Journal of Emerging and Selected Topics in Power Electronics

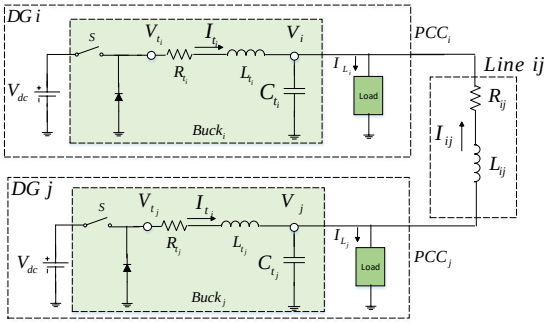

Fig. 1. Electrical scheme of islanded DC microgrid consisted of two DGs.

optimization problem that leads to an optimal controller and therefore, an optimal performance.

- Unlike [25] and [26], the design of this control system allows us to apply no constraint on Lyapunov matrices to achieve a decentralized strategy. Therefore, it results in less conservatism.
- Contrary to [24]-[27], the robust performance property of the developed control system eliminates the need for the development of pre-filters, which reduces the computational complexity of the controller.

To evaluate the efficiency of the developed robust voltage controller, various scenarios are executed using SimPowerSystems Toolbox in MATLAB. The results of these simulations prove the efficiency of the presented control system.

The organization of this paper is as follows. The dynamical model of the islanded DC microgrid system is presented in section II. The decentralized robust H_∞ voltage control system is developed in section III. The effectiveness of the controller is analyzed by simulating various case studies in section IV. The experimental validation of the proposed control method is presented in section V. Section VI concludes the paper.

Throughout the paper, the set of real numbers, the identity, and the zero matrices are indicated by $\Re$, I, and 0, respectively. For a given matrix S, the transpose, the inverse, and the inverse transpose of S, are respectively denoted by S^T, S^{-1}, S^{-T}. Also, the symbol $*$ indicate a symmetric block in a matrix.

II. Autonomous DC Microgrid Modelling

In this section, the state-space dynamical model of a DC microgrid composed of multiple DG units operating in islanding mode is represented. First, we derive the model of an autonomous DC microgrid consisted of two DGs, then we generalize the model to a multi-DG microgrid system. Contrary to the previous researches and in order for the controller to be applicable on DC microgrids with different topologies, we have considered a general topology for the DC microgrid in this research. In this way, every DG unit is comprised of a local load and each DG unit has the possibility to be connected to any other DG unit through a distribution line. In this way, the proposed control system is applicable to DC microgrids with parallel, radial or meshed topology.

Consider the electrical scheme illustrated in Fig. 1. In this model, each DG unit comprises a DC voltage source and a DC-DC converter that are connected to a local load with an unknown parameter and topology. As it is shown in Fig. 1, we used the buck converter as the DC-DC converter with d_{buck} as its duty cycle in our design. However, if the converter type is boost, the appropriate model must be replaced. Using the buck converter model in [28], the dynamical model of DG i and distribution line ij can be demonstrated respectively as bellow:

$$\begin{aligned}\frac{dV_i}{dt} &= \frac{1}{C_{t_i}}I_{t_i} - \frac{1}{C_{t_i}}I_{L_i} + \frac{1}{C_{t_i}}I_{ij}\\ \frac{dI_{t_i}}{dt} &= -\frac{1}{L_{t_i}}V_i - \frac{R_{t_i}}{L_{t_i}}I_{t_i} + \frac{d_{buck_i}}{L_{t_i}}V_{dc_i}\end{aligned} \tag{1}$$

$$\frac{dI_{ij}}{dt} = -\frac{R_{ij}}{L_{ij}}I_{ij} + \frac{1}{L_{ij}}V_j - \frac{1}{L_{ij}}V_i \tag{2}$$

where V_i, I_{t_i}, I_{L_i}, and $I_{L_{ij}}$ are the PCC voltage, filter current, load current, and the distribution line current, respectively.

A. Quasi-Stationary Lines (QSL) Approximated Model

To simplify the equations and to achieve a neutral interaction between DG units, the QSL approximation of the line dynamics are used in the modelling process. It should be noted that since the impedance of the lines in the DC microgrid is mostly resistive, the assumption of QSL is reasonable.

Using the QSL approximated model presented in [29], we set $\frac{dI_{ij}}{dt} = 0$ in equation (2). Therefore, $I_{ij} = \frac{V_j - V_i}{R_{ij}}$. Now by replacing this value with the I_{ij} in (1), we have:

$$\begin{aligned}\frac{dV_i}{dt} &= \frac{1}{C_{t_i}}I_{t_i} - \frac{1}{C_{t_i}}I_{L_i} + \frac{1}{C_{t_i}R_{ij}}V_j - \frac{1}{C_{t_i}R_{ij}}V_i\\ \frac{dI_{t_i}}{dt} &= -\frac{1}{L_{t_i}}V_i - \frac{R_{t_i}}{L_{t_i}}I_{t_i} + \frac{d_{buck_i}}{L_{t_i}}V_{dc_i}\end{aligned} \tag{3}$$

Therefore, the state-space representation of DG i linked to DG j through distribution line ij can be described as follows:

$$\begin{aligned}\dot{x}_{g_i} &= A_{g_{ii}}x_{g_i} + A_{g_{ij}}x_{g_j} + B_{g_i}u_i + B_{d_i}d_i\\ y_i &= C_{g_i}x_{g_i}\end{aligned} \tag{4}$$

where $x_{g_i} = \begin{bmatrix}V_i & I_{t_i}\end{bmatrix}^T$, $u_i = d_{buck_i}v_{dc_i}$, $d_i = I_{L_i}$, and $y_i = V_i$ are the state, input, exogenous input, and output vectors of DG i, respectively. The state-space matrices of (4) are represented as bellow:

$$\begin{aligned}A_{g_{ii}} &= \begin{bmatrix}-\frac{1}{C_{t_i}R_{ij}} & \frac{1}{C_{t_i}}\\ -\frac{1}{L_{t_i}} & -\frac{R_{t_i}}{L_{t_i}}\end{bmatrix}, \quad A_{g_{ij}} = \begin{bmatrix}\frac{1}{R_{ij}C_{t_i}} & 0\\ 0 & 0\end{bmatrix}\\ B_{g_i} &= \begin{bmatrix}0\\ \frac{1}{L_{t_i}}\end{bmatrix}, \quad B_{d_i} = \begin{bmatrix}-\frac{1}{C_{t_i}}\\ 0\end{bmatrix}, \quad C_{g_i} = \begin{bmatrix}1 & 0\end{bmatrix}\end{aligned} \tag{5}$$

B. Generalized Model of an Autonomous DC Microgrid with Multiple DGs

Now we consider a DC microgrid system consists of multiple DG units. Assuming that N_i is a subset that contains the indices of the neighbors of DG i, where

This article has been accepted for publication in a future issue of this journal, but has not been fully edited. Content may change prior to final publication. Citation information: DOI 10.1109/JESTPE.2021.3054723, IEEE Journal of Emerging and Selected Topics in Power Electronics

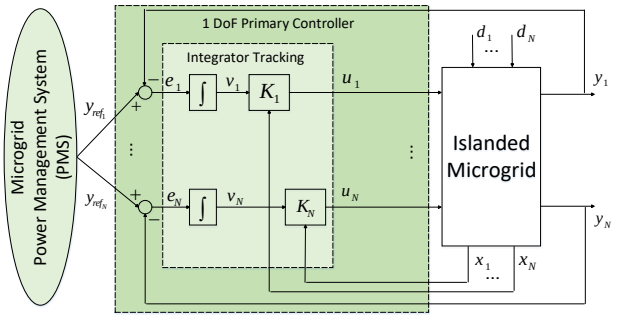

Fig. 2. Islanded DC microgrid control system with integrator tracking.

$N_i \subset \{1 \quad \dots \quad N\}$, we can simply generate model (4) to a microgrid system with multiple DG units as bellow [25]:

$$\begin{aligned} \dot{x}_{g_i} &= A_{g_{ii}} x_{g_i} + \sum_{j \in N_i} A_{g_{ij}} x_{g_j} + B_{g_i} u_i + B_{d_i} d_i \\ y_i &= C_{g_i} x_{g_i}; \quad i = 1, \dots, N \end{aligned} \tag{6}$$

where

$$\begin{aligned} A_{g_{ii}} &= \begin{bmatrix} -\sum_{j \in N_i} \frac{1}{C_{t_i} R_{ij}} & \frac{1}{C_{t_i}} \\ -\frac{1}{L_{t_i}} & -\frac{R_{t_i}}{L_{t_i}} \end{bmatrix}, A_{g_{ij}} = \begin{bmatrix} \frac{1}{R_{ij} C_{t_i}} & 0 \\ 0 & 0 \end{bmatrix} \\ B_{g_i} &= \begin{bmatrix} 0 \\ \frac{1}{L_{t_i}} \end{bmatrix}, \quad B_{d_i} = \begin{bmatrix} -\frac{1}{C_{t_i}} \\ 0 \end{bmatrix}, \quad C_{g_i} = \begin{bmatrix} 1 & 0 \end{bmatrix} \end{aligned} \tag{7}$$

III. Islanded DC Microgrid Control Strategy

Fig. 2 illustrates the proposed non-droop-based hierarchical control for the islanded operation of DC microgrids, which consists of two levels. The primary control level is accountable for fast voltage regulation and correcting the voltage steady-state deviations. Primary control level is based on a decentralized control strategy that operates based on local measurements and do not require any sort of communications. As the result, the need for communication channels as well as problems such as delay, communication link failure, etc., that arise in control methods based on non-decentralized control structure is eliminated. Compared to the droop-based hierarchical control strategy, there is no voltage steady-state error in the primary level of non-droop based control strategy and therefore, there is no need for another level to compensate the voltage deviations. The PMS is responsible for preserving the optimal operating point in the second control level, commonly based on a cost function corresponding to every DG unit and then broadcasting respective voltage set-pints to the primary level [15]. The focus of this paper is to develop a one DoF optimal robust voltage control system for the primary level of the hierarchical control strategy for the autonomous DC microgrid considering various sources of uncertainty, with the following objectives:

1) Decentralized structure of the controller, such that no communication is needed.
2) Asymptotic stability of the overall closed-loop system.
3) Asymptotic tracking of the voltage references.
4) Desired transient performance of the microgrid system.
5) Robust performance and robust stability of the closed-loop microgrid concerning PnP operation, topological changes, load changes, different subsequent system changes, and presence of the CPLs.

A. Voltage Tracking

To have a precise voltage tracking at the PCC of all DGs, each unit is augmented using an integrator as bellow:

$$\dot{v}_i = e_i = y_{ref_i} - y_i = y_{ref_i} - C_{g_i} x_{g_i} \tag{8}$$

hence, the augmented islanded DC microgrid is represented as follows:

$$\begin{aligned} \dot{\hat{x}}_{g_i} &= \hat{A}_{g_{ii}} \hat{x}_{g_i} + \sum_{j \in N_i} \hat{A}_{g_{ij}} \hat{x}_{g_j} + \hat{B}_{g_i} u_i + \hat{B}_{d_i} \hat{d}_i \\ \hat{y}_i &= \hat{C}_{g_i} \hat{x}_{g_i} \end{aligned} \tag{9}$$

where $\hat{x}_{g_i} = \begin{bmatrix} V_i & I_{t_i} & v_i \end{bmatrix}^T$, $\hat{y}_i = \begin{bmatrix} y_i & v_i \end{bmatrix}^T$, $\hat{d}_i = \begin{bmatrix} I_{L_i} & V_{ref_i} \end{bmatrix}^T$, and

$$\begin{aligned} \hat{A}_{g_{ii}} &= \begin{bmatrix} A_{g_{ii}} & 0 \\ -C_{g_{ii}} & 0 \end{bmatrix}, \quad \hat{A}_{g_{ij}} = \begin{bmatrix} A_{g_{ij}} & 0 \\ 0 & 0 \end{bmatrix}, \\ \hat{B}_{g_i} &= \begin{bmatrix} B_{g_i} \\ 0 \end{bmatrix}, \quad \hat{B}_{d_i} = \begin{bmatrix} B_{d_i} & 0 \\ 0 & I \end{bmatrix}, \\ \hat{C}_{g_i} &= \begin{bmatrix} C_{g_i} & 0 \\ 0 & I \end{bmatrix} \end{aligned} \tag{10}$$

B. Microgrid PnP Functionality and Topology Changes Modelling

The discontinuous nature of renewable energy resources causes the plugging-in and/or out of the DG units in a microgrid system, which can disrupt the stability of the DC microgrid and even lead to instability.

A closer look at the DC microgrid system state-space matrices in (7), shows that the plugging-in and/or out of DGs to/from DG i, only affects matrix $A_{g_{ii}}$ and as a result, the augmented matrix $\hat{A}_{g_{ii}}$ in (10). Therefore, we will consider two cases for every DG unit.

1) No connection between DG i and other DGs, and therefore no value for $\sum_{j \in N_i} \frac{1}{C_{t_i} R_{(ij)}}$, i.e. 0.
2) Maximum possible connections between DG i and other DGs and therefore $\sum_{j \in N_i} \frac{1}{C_{t_i} R_{(ij)}} = \sum_{j \in N_{i_{max}}} \frac{1}{C_{t_i} R_{ij}}$.

corresponding matrices $\hat{A}_{g_{ii}}$ for the two cases are described as bellow:

$$\begin{aligned} \hat{A}^1_{g_{ii}} &= \begin{bmatrix} 0 & \frac{1}{C_{t_i}} & 0 \\ -\frac{1}{L_{t_i}} & -\frac{R_{t_i}}{L_{t_i}} & 0 \\ 1 & 0 & 0 \end{bmatrix} \\ \hat{A}^2_{g_{ii}} &= \begin{bmatrix} -\sum_{j \in N_{i_{max}}} \frac{1}{C_{t_i} R_{ij}} & \frac{1}{C_{t_i}} & 0 \\ -\frac{1}{L_{t_i}} & -\frac{R_{t_i}}{L_{t_i}} & 0 \\ 1 & 0 & 0 \end{bmatrix} \end{aligned} \tag{11}$$

If we consider the two vertices in (11) as two points, all the possible cases for connection or disconnection of DG units to/from DG i will belong to a polytopic zone as bellow:

$$\hat{A}_{g_{ii}}(\lambda) = \sum_{v=1}^{2} \lambda_v \hat{A}^v_{g_{ii}}, \quad 0 \leq \lambda \leq 1 \tag{12}$$

This article has been accepted for publication in a future issue of this journal, but has not been fully edited. Content may change prior to final publication. Citation information: DOI 10.1109/JESTPE.2021.3054723, IEEE Journal of Emerging and Selected Topics in Power Electronics

It is important to note that the stated polytopic uncertainty also covers the topological changes of the system (disconnection of some of the distribution lines) and therefore, this approach also provides robustness to the topology changes.

Also, It is worth to mention that using theorem 1 in the following subsection, the effect of interaction matrix $A_{g_{ij}}$ on the control system can be neglected. therefore, the effect of PnP operation on matrix $A_{g_{ij}}$ is neglected.

C. Robust Control System

In this section, an optimal one DoF robust control system with a decentralized strategy is designed for the islanded operation of uncertain DC microgrids.The objective contrary to the previous researches is to not only provide robust stability, but also to provide optimal robust desired performance for the DC microgrid system by developing a unique optimization problem.

1) State-Feedback Design: Consider the state-space model of the augmented DG i with z_i as its corresponding controlled output as bellow:

$$\begin{aligned}\dot{\hat{x}}_{g_i} &= \hat{A}_{g_{ii}}(\lambda)\hat{x}_{g_i} + \sum_{j\in N_i}\hat{A}_{g_{ij}}\hat{x}_{g_j} + \hat{B}_{g_i}u_i + \hat{B}_{d_i}\hat{d}_i \\ \hat{y}_i &= \hat{C}_{g_i}\hat{x}_{g_i} \\ z_i &= C_{2g_i}\hat{x}_{g_i} + D_{g_i}u_i + D_{d_i}\hat{d}_i\end{aligned} \tag{13}$$

To attain a desirable time-domain performance concerning tracking the voltage set-points and minimizing the effect of disturbances on the output voltages, we consider $z_i = \begin{bmatrix} e_i & V_i \end{bmatrix}^T$ as the controlled output vector.

The goal is to develop a one DoF robust state-feedback controller for the augmented DC microgrid in (13) using the following control law such that the robust stability and the robust H_∞ performance of the overall islanded DC microgrid are guaranteed.

$$u_i = K_i\hat{x}_{g_i} \tag{14}$$

Using the control law in (14), we have the closed-loop system as bellow:

$$\begin{aligned}\dot{\hat{x}}_{g_i} &= (\hat{A}_{g_{ii}}(\lambda) + \hat{B}_{g_i}K_i)\hat{x}_{g_i} + \sum_{j\in N_i}\hat{A}_{g_{ij}}\hat{x}_{g_j} + \hat{B}_{d_i}\hat{d}_i \\ \hat{y}_i &= \hat{C}_{g_i}\hat{x}_{g_i} \\ z_i &= (C_{2g_i} + D_{g_i}K_i)\hat{x}_{g_i} + D_{d_i}\hat{d}_i\end{aligned} \tag{15}$$

The overall closed-loop DC microgrid system can be described as bellow:

$$\begin{aligned}\dot{\hat{x}} &= (\hat{A}(\lambda) + \hat{B}_gK)\hat{x} + \hat{B}_d\hat{d} \\ \hat{y} &= \hat{C}_g\hat{x} \\ z &= (C_{2g} + D_gK)\hat{x} + D_d\hat{d}\end{aligned} \tag{16}$$

in above, $\hat{x} = \begin{bmatrix}\hat{x}_{g_1}^T & \dots & \hat{x}_{g_N}^T\end{bmatrix}^T$, $\hat{d} = \begin{bmatrix}\hat{d}_1^T & \dots & \hat{d}_N^T\end{bmatrix}^T$, $\hat{y} = \begin{bmatrix}\hat{y}_1^T & \dots & \hat{y}_N^T\end{bmatrix}^T$, $z = \begin{bmatrix}z_1^T & \dots & z_N^T\end{bmatrix}^T$, and

$$\begin{aligned}\hat{A}(\lambda) &= \begin{bmatrix}\hat{A}_{g_{11}}(\lambda) & \hat{A}_{g_{12}} & \cdots & \hat{A}_{g_{1N}} \\ \hat{A}_{g_{21}} & \hat{A}_{g_{22}}(\lambda) & \cdots & \hat{A}_{g_{2N}} \\ \vdots & \vdots & \ddots & \vdots \\ \hat{A}_{g_{N1}} & \hat{A}_{g_{N2}} & \cdots & \hat{A}_{g_{NN}}(\lambda)\end{bmatrix} \\ \hat{B}_g &= diag(\hat{B}_{g_1},\dots,\hat{B}_{g_N}) \quad \hat{B}_d = diag(\hat{B}_{d_1},\dots,\hat{B}_{d_N}) \\ \hat{C}_g &= diag(\hat{C}_{g_1},\dots,\hat{C}_{g_N}) \quad C_{2g} = diag(C_{2g_1},\dots,C_{2g_N}) \\ D_g &= diag(D_{g_1},\dots,D_{g_N}) \quad D_d = diag(D_{d_1},\dots,D_{d_N}) \\ K &= diag(K_1,\dots,K_N)\end{aligned} \tag{17}$$

As is clear in (15), terms $\sum_{j\in N_i}\hat{A}_{g_{ij}}\hat{x}_{g_j}$ prevent the decentralized design of the control system. Therefore, conditions must be considered to neutralize the effect of these interaction terms and to guaranty the stability of the overall closed-loop DC microgrid by stabilizing all the subsystems. To that end, we present the following theorem that assigns the conditions to the design of the robust H_∞ control system, such that the stability of all the DG units guarantee the stability of the overall closed-loop DC microgrid. The state-feedback gains K_i are developed using the following theorem.

Theorem 1. *Assuming $\epsilon_i \neq 0, \zeta_i \in (-1,1)$, and $\gamma > 0$, if Lyapunov matrices $W_i^v = {W_i^v}^T \in \Re^{n_x\times n_x}$, and slack matrices $X_i \in \Re^{n_x\times n_x}$ and $Z_i \in \Re^{n_u\times n_x}$ exist, such that:*

$$\begin{bmatrix} W_i^v + \Psi_i^v + \Psi_i^{vT} & * & * & * \\ \zeta_i\Psi_i^{v^T} - \bar{A}_{g_{ii}}^v X_i - \bar{B}_{g_i}Z_i & \Upsilon_i^v & * & * \\ B_{d_i}^T & -\bar{B}_{g_i}^T & -I & * \\ \Gamma_i & \zeta_i\Gamma_i & D_{d_i} & -\gamma I \end{bmatrix} < 0 \tag{18}$$

where

$$\begin{aligned}\Psi_i^v &= \tilde{A}_{g_{ii}}^v X_i + \bar{B}_{g_i}Z_i, \quad \Gamma_i = C_{2g_i}X_i + D_{g_i}Z_i \\ \Upsilon_i^v &= -W_i^v - \zeta_i\bar{A}_{g_{ii}}^v X_i - \zeta_i\bar{B}_{g_i}Z_i - \zeta_i X_i^T\bar{A}_{g_{ii}}^{v^T} - \zeta_i Z_i^T\hat{B}_{g_i}^T \\ \tilde{A}_{g_{ii}}^v &= \epsilon_i\hat{A}_{g_{ii}}^v - 1/2\epsilon_i, \quad \bar{A}_{g_{ii}}^v = \epsilon_i\hat{A}_{g_{ii}}^v - 1/2\epsilon_i \\ \bar{B}_{g_i} &= \epsilon_i\hat{B}_{g_i}, \quad \bar{B}_{d_i} = \epsilon_i\hat{B}_{d_i}\end{aligned} \tag{19}$$

and the structure of the slack matrix X_i is fixed as bellow:

$$X_i = \left[\begin{array}{c|c} \eta_i & 0_{1\times 2} \\ \hline X_{21_i} & X_{22_i}\end{array}\right] \tag{20}$$

where $\eta_i > 0$, and i and v are the DGs, and the polytopic uncertainty vertice numbers, respectively. And $\eta_i > 0$ must be chosen such that $\eta_i/R_{ij}C_i \simeq 0$ holds for every DG unit. Then the state-feedback gains $K_i = Z_iX_i^{-1}$ guaranty the robust stability and robust H_∞ performance of the overall closed-loop DC microgrid system with $\|z_i/\hat{d}_i\|_\infty \ll \sqrt{\gamma}$.

Proof. Check Appendix. □

2) CPLs: Another challenge in the stability analysis of DC microgrid systems is the presence of CPLs. CPLs require constant power, irrespective of the system input voltage. The input current in CPLs decreases once the input voltage increases (and vice versa). Consequently, CPLs can represent

This article has been accepted for publication in a future issue of this journal, but has not been fully edited. Content may change prior to final publication. Citation information: DOI 10.1109/JESTPE.2021.3054723, IEEE Journal of Emerging and Selected Topics in Power Electronics

negative impedance [32]. To obtain constraints that allow the control system to maintain its optimal performance against CPLs, the dynamical model of the autonomous DC microgrid is calculated once again considering the presence of CPLs. It is considered that a CPL with the constant power of P_{CPL} is connected to DG i as bellow:

$$\begin{aligned}\frac{dV_i}{dt} &= \frac{1}{C_{t_i}} I_{t_i} - \frac{1}{C_{t_i}} I_{CPL_i} + \sum_{j\in N_i} \frac{1}{C_{t_i} R_{ij}} (V_j - V_i) \\ \frac{dI_{t_i}}{dt} &= -\frac{1}{L_{t_i}} V_i - \frac{R_{t_i}}{L_{t_i}} I_{t_i} + \frac{d_{buck_i}}{L_{t_i}} V_{dc_i}\end{aligned} \tag{21}$$

Assuming that the system (21) has equilibrium points $(\bar{V}_i, \bar{V}_j, \bar{I}_{t_i}, \bar{d}_{buck_i})$, such that:

$$\begin{aligned}0 &= \frac{1}{C_{t_i}} \bar{I}_{t_i} - \frac{1}{C_{t_i}} \bar{I}_{CPL_i} + \sum_{j\in N_i} \frac{1}{C_{t_i} R_{ij}} (\bar{V}_j - \bar{V}_i) \\ 0 &= -\frac{1}{L_{t_i}} \bar{V}_i - \frac{R_{t_i}}{L_{t_i}} \bar{I}_{t_i} + \frac{\bar{d}_{buck_i}}{L_{t_i}} V_{dc_i}\end{aligned} \tag{22}$$

linearization of (21) around its equilibrium points, results in a linear model as bellow:

$$\begin{aligned}\begin{bmatrix}\dot{\tilde{V}}_i \\ \dot{\tilde{I}}_{t_i}\end{bmatrix} = &\begin{bmatrix}-\frac{1}{C_{t_i}} \sum_{j\in N_i} (\frac{1}{R_{ij}} - \frac{P_{CPL}}{\bar{V}_i^2}) & \frac{1}{C_{t_i}} \\ -\frac{1}{L_{t_i}} & -\frac{R_{t_i}}{L_{t_i}}\end{bmatrix} \begin{bmatrix}\tilde{V}_i \\ \tilde{I}_{t_i}\end{bmatrix} + \\ &\sum_{j\in N_i} \begin{bmatrix}\frac{1}{R_{ij} C_{t_i}} & 0 \\ 0 & 0\end{bmatrix} \begin{bmatrix}\tilde{V}_j \\ \tilde{I}_{t_j}\end{bmatrix} + \begin{bmatrix}0 \\ \frac{1}{L_{t_i}}\end{bmatrix} \tilde{d}_{buck_i} V_{dc_i}\end{aligned} \tag{23}$$

where $\tilde{V}_i = V_i - \bar{V}_i, \tilde{I}_{t_i} = I_{t_i} - \bar{I}_{t_i}, \tilde{V}_j = V_j - \bar{V}_j, \tilde{I}_{t_j} = I_{t_j} - \bar{I}_{t_j}$, and $\tilde{d}_{buck_i} = d_{buck_i} - \bar{d}_{buck_i}$.

The control law for the system is $\tilde{d}_{buck_i} V_{dc_i} = \begin{bmatrix}K_{i_1} & K_{i_2}\end{bmatrix} \begin{bmatrix}\tilde{V}_i \\ \tilde{I}_{t_i}\end{bmatrix}$. As the result, the closed-loop system can be defined as follows:

$$A_{cl_i} = \begin{bmatrix}-\frac{1}{C_{t_i}} \sum_{j\in N_i} (\frac{1}{R_{ij}} - \frac{P_{CPL}}{\bar{V}_i^2}) & \frac{1}{C_{t_i}} \\ -\frac{1-K_{i_1}}{L_{t_i}} & -\frac{R_{t_i}-K_{i_2}}{L_{t_i}}\end{bmatrix} \tag{24}$$

The closed-loop DC microgrid (24) is stable, if and only if $trace(A_{cl_i}) < 0$ and $det(A_{cl_i}) > 0$. Therefore, constraints that allow the control system to maintain the microgrid optimal performance under CPLs are as follow:

$$\begin{aligned}K_{i_1} &< (\sum_{j\in N_i} \frac{1}{R_{ij}} - \frac{P_{CPL}}{\bar{V}_i^2})(R_{t_i} - K_{i_2}) + 1 \\ K_{i_2} &< \frac{L_{t_i}}{C_{t_i}} (\sum_{j\in N_i} \frac{1}{R_{ij}} - \frac{P_{CPL}}{\bar{V}_i^2}) + R_{t_i}\end{aligned} \tag{25}$$

3) Algorithm for the Controller Design: In the following, a step-by-step algorithm is presented to design the one DoF optimal robust controller for every DG in the islanded DC microgrid.

Step1: Form the two vertices $\hat{A}^1_{g_{ii}}$ and $\hat{A}^2_{g_{ii}}$ as in (11).

Step2: Apply the structure specified in (20) for slack matrices X_i.

Step3: Fix the scalar parameters $\epsilon_i \neq 0$, $\zeta_i \in (-1, 1)$, and $\gamma > 0$, and then solve the following convex optimization problem to calculate the state-feedback gains.

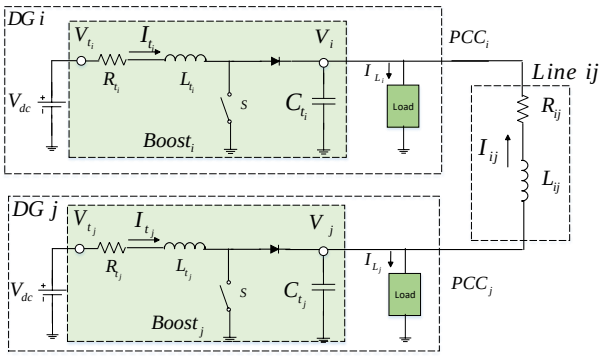

Fig. 3. Average model of DGs with boost converter.

$$\begin{aligned}&\min_{W_i^v, X_i, Z_i} \ \eta_i \\ &\begin{bmatrix}W_i^v + \Psi_i^v + \Psi_i^{v^T} & * & * & * \\ \zeta_i \Psi^T - \bar{A}^v_{g_{ii}} X_i - \bar{B}_{g_i} Z_i & \Upsilon_i^v & * & * \\ B_{d_i}^T & -\bar{B}_{g_i}^T & -I & * \\ \Gamma_i & \zeta_i \Gamma_i & D_{d_i} & -\gamma I\end{bmatrix} < 0 \\ &\Psi_i^v = \tilde{A}^v_{g_{ii}} X_i + \bar{B}_{g_i} Z_i, \quad \Gamma_i = C_{2g_i} X_i + D_{g_i} Z_i \\ &\Upsilon_i^v = -W_i^v - \zeta_i \bar{A}^v_{g_{ii}} X_i - \zeta_i \bar{B}_{g_i} Z_i - \zeta_i X_i^T \bar{A}^{v^T}_{g_{ii}} - \zeta_i Z_i^T \bar{B}_{g_i}^T \\ &\tilde{A}^v_{g_{ii}} = \epsilon_i \hat{A}^v_{g_{ii}} - 1/2\epsilon_i, \quad \bar{A}^v_{g_{ii}} = \epsilon_i \hat{A}^v_{g_{ii}} - 1/2\epsilon_i \\ &\bar{B}_{g_i} = \epsilon_i \hat{B}_{g_i}, \quad \bar{B}_{d_i} = \epsilon_i \hat{B}_{d_i} \\ &K_{i_1} < (\sum_{j\in N_i} \frac{1}{R_{ij}} - \frac{P_{CPL}}{\bar{V}_i^2})(R_{t_i} - K_{i_2}) + 1 \\ &K_{i_2} < \frac{L_{t_i}}{C_{t_i}} (\sum_{j\in N_i} \frac{1}{R_{ij}} - \frac{P_{CPL}}{\bar{V}_i^2}) + R_{t_i} \\ &\quad i = 1, \ldots, N; \quad v = 1, 2.\end{aligned} \tag{26}$$

D. Voltage Controller in case of Using Boost Converter

If we use boost converter with the average model illustrated in Fig. 3, DG i with N_i as a subset that contains the indices of the neighbors of DG i is mathematically described as bellow:

$$\begin{aligned}\frac{dV_i}{dt} &= \frac{1 - d_{boost_i}}{C_{t_i}} I_{t_i} - \frac{I_{L_i}}{C_{t_i}} + \frac{1}{C_{t_i}} \sum_{j\in N_i} \frac{V_j - V_i}{R_{ij}} \\ \frac{dI_{t_i}}{dt} &= -\frac{1 - d_{boost_i}}{L_{t_i}} V_i - \frac{R_{t_i}}{L_{t_i}} I_{t_i} + \frac{1}{L_{t_i}} V_{dc_i}\end{aligned} \tag{27}$$

where d_{boost_i} is the duty cycle of the boost converter in DG i. However, due to the presence of two bilinear terms $(1 - d_{boost_i}) I_{t_i}$ and $(1 - d_{boost_i}) V_i$, the model (27) is not linear. Linearization of (27) around fixed points $(\bar{V}_i, \bar{V}_j, \bar{I}_{t_i}, \bar{I}_{L_i}, \bar{d}_{boost_i})$ results in the following model:

$$\begin{aligned}\frac{d}{dt} \begin{bmatrix}\tilde{V}_i \\ \tilde{I}_{t_i}\end{bmatrix} \approx &\begin{bmatrix}-\frac{1}{C_{t_i}} \sum_{j\in N_i} \frac{1}{R_{ij}} & \frac{1 - \bar{d}_{boost_i}}{C_{t_i}} \\ -\frac{1 - \bar{d}_{boost_i}}{L_{t_i}} & -\frac{R_{t_i}}{L_{t_i}}\end{bmatrix} \begin{bmatrix}\tilde{V}_i \\ \tilde{I}_{t_i}\end{bmatrix} \\ &+ \sum_{j\in N_i} \begin{bmatrix}\frac{1}{R_{ij} C_{t_i}} & 0 \\ 0 & 0\end{bmatrix} \begin{bmatrix}\tilde{V}_j \\ \tilde{I}_{t_j}\end{bmatrix} + \begin{bmatrix}-\frac{1}{C_{t_i}} \\ 0\end{bmatrix} \tilde{I}_{L_i} + \begin{bmatrix}-\frac{\bar{I}_{t_i}}{C_{t_i}} \\ \frac{\bar{V}_i}{L_{t_i}}\end{bmatrix} \tilde{d}_{boost_i}\end{aligned} \tag{28}$$

This article has been accepted for publication in a future issue of this journal, but has not been fully edited. Content may change prior to final publication. Citation information: DOI 10.1109/JESTPE.2021.3054723, IEEE Journal of Emerging and Selected Topics in Power Electronics

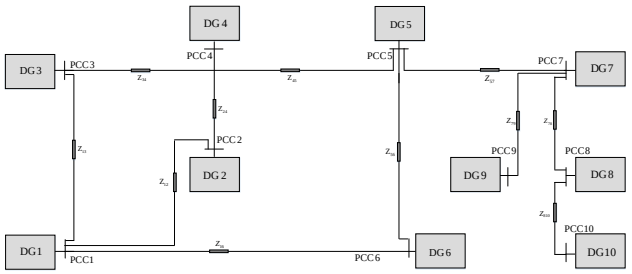

Fig. 4. Schematic diagram of an islanded DC microgrid with 10 DG units.

where $\tilde{V}_i = V_i - \bar{V}_i, \tilde{I}_{t_i} = I_{t_i} - \bar{I}_{t_i}, \tilde{V}_j = V_j - \bar{V}_j, \tilde{I}_{L_i} = I_{L_i} - \bar{I}_{L_i}$, and $\tilde{d}_{boost_i} = d_{boost_i} - \bar{d}_{boost_i}$. The model can be presented exactly as the state-space model (6) with following state-space matrices.

$$A_{g_{ii}} = \begin{bmatrix} -\frac{1}{C_{t_i}} \sum_{j \in N_i} \frac{1}{R_{ij}} & \frac{1-\bar{d}_{boost_i}}{C_{t_i}} \\ -\frac{1-\bar{d}_{boost_i}}{L_{t_i}} & -\frac{R_{t_i}}{L_{t_i}} \end{bmatrix},$$
$$A_{g_{ij}} = \begin{bmatrix} \frac{1}{R_{ij}C_{t_i}} & 0 \\ 0 & 0 \end{bmatrix} \quad B_{g_i} = \begin{bmatrix} -\frac{\bar{I}_{t_i}}{C_{t_i}} \\ \frac{\bar{V}_i}{L_{t_i}} \end{bmatrix}, \quad B_{d_i} = \begin{bmatrix} -\frac{1}{C_{t_i}} \\ 0 \end{bmatrix},$$
$$C_{g_i} = \begin{bmatrix} 1 & 0 \end{bmatrix} \tag{29}$$

All the other equations remain unchanged and therefore, the proposed voltage control strategy can be applied to DGs with boost converter modeled as (6) and (29). This approach is the same in case of any other converter.

IV. Simulation Results

This section is devoted to evaluating the efficiency of the developed robust control system. The simulations are conducted on the islanded DC microgrid depicted in Fig. 4, which is consisted of 10 DG units with general topology. The local controllers are developed for all the DGs using the step-by-step algorithm presented in the previous section. DGs and distribution lines parameters are determined in Tables I and II, respectively. All the parameters are based on the models presented in previous researches, which have been widely used to evaluate the performance of non-droop-based controllers [16], [17], [24], and [25]. State-feedback gains are calculated by solving the convex optimization problem (26) using YALMIP [33] as the interface and SEDUMI [34] as the solver. The simulations were run on a PC with Intel(R) Core(TM) i5-2450M CPU @2.50GHz and 8.00GB memory.

In order for the simulations to be performed based on real-time simulation considerations, and to demonstrate the practical applicability of the designed control algorithm, all the simulations have been performed in a discrete-time simulation environment. In practice, the sampling frequency should be chosen at least twice as fast as the switching frequency of power electronics components [35]. Therefore, the switching frequency and the sampling frequency of the system have been chosen as $10KHz$ and $20KHz$, respectively, which are reasonable for typical real-time digital simulators (RTDSs) [36]. Also, it is worth to mention that the sampling frequency of the closed-loop system is identical for each local controller in the microgrid system.

TABLE I
Microgrid DG Units Parameter Values

DGs	$R_t(\Omega)$	$L_t(mH)$	$C_t(mF)$	$R_L(\Omega)$	$P_{CPL}(W)$	$V_{ref}(V)$
DG 1	0.2	1.8	2.2	10	125	47.9
DG 2	0.3	2.0	1.9	6	140	48
DG 3	0.1	2.2	1.7	4	115	47.7
DG 4	0.5	3.0	2.5	2	135	48
DG 5	0.4	1.2	2.0	3	100	47.8
DG 6	0.6	2.5	3.0	8	120	48.1
DG 7	0.5	2.0	1.9	6	115	47.8
DG 8	0.4	2.5	2.2	4	125	48.2
DG 9	0.6	3.0	2.0	7	130	48
DG 10	0.3	1.5	3.0	8	120	47.7

DC Bus Voltage	$V_{dc} = 100V$
Switching Frequency	$f_{sw} = 10KHz$
System Nominal Frequency	$f_0 = 60Hz$
Sampling Frequency	$f_s = 20KHz$

TABLE II
Parameters Values of Distribution Lines

Z_{ij}	$R_{ij}(\Omega)$	$L_{ij}(\mu H)$
Z_{12}	0.05	2.1
Z_{13}	0.07	1.8
Z_{34}	0.06	1.0
Z_{24}	0.04	2.3
Z_{45}	0.08	1.8
Z_{16}	0.1	2.5
Z_{56}	0.08	3.0
Z_{57}	0.06	2.0
Z_{78}	0.05	2.2
Z_{79}	0.07	1.8
Z_{810}	0.06	3.0

A. Scenario 1: Voltage Tracking

In the first scenario, we analyze the efficiency of the control system in tracking voltage reference signals. The reference voltages for all the DG units are set according to the values illustrated in Table I.

Based on IEEE standards in [37], the control system must provide stability, desired transient, and desired steady-state performance for the closed-loop DC microgrid system. To analyze the fulfilment of the mentioned requirements with respect to tracking voltage references, the reference voltages of DG 1 and DG 9 are simultaneously changed from $47.9V$ to $48.5V$ and from $48V$ to $47.5V$ at $t = 1s$, respectively. The performance of the developed control system regarding these voltage reference changes is illustrated in Fig. 5. Fig. 5(a)and Fig. 5(f) illustrate the behavior of the output voltages of DG 1 and DG 9 and prove that the proposed controller provides stability and desired performance for the closed-loop DC microgrid. Furthermore, the stability and desired

This article has been accepted for publication in a future issue of this journal, but has not been fully edited. Content may change prior to final publication. Citation information: DOI 10.1109/JESTPE.2021.3054723, IEEE Journal of Emerging and Selected Topics in Power Electronics

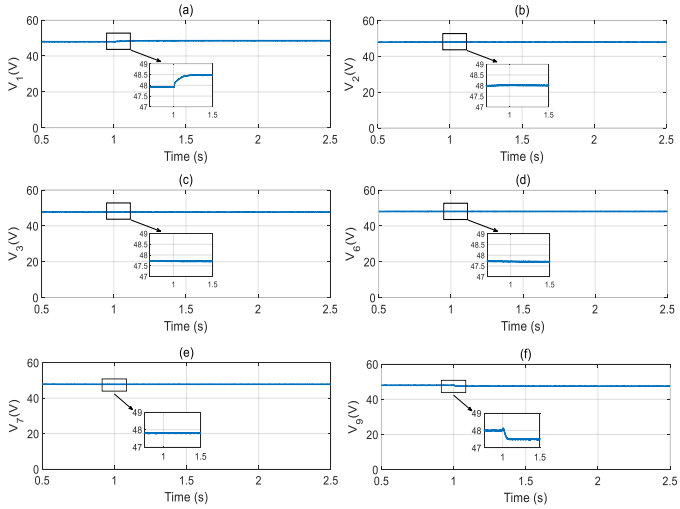

Fig. 5. Performance of the microgrid system concerning DG 1 and DG 9 voltage reference changing: (a) output voltage of DG 1, (b) output voltage of DG 2, (c) output voltage of DG 3, (d) output voltage of DG 6, (e) output voltage of DG 7, (f) output voltage of DG 9.

performance are robust against reference values changes and the local controllers effectively regulate the output voltages with a very small transient and with zero steady-state error according to the IEEE standards in [37]. Also, the dynamical behaviors of neighboring DGs of DG 1 and DG 9 (i.e. DGs 2, 3, 6, and 7) are illustrated in Fig. 5(b), 5(c), 5(d), and 5(e), respectively. Robustness of stability and performance of these neighboring DGs with zero steady-state error is confirmed in these results.

B. Scenario 2: PnP Functionality of DGs

As mentioned earlier, due to the discontinuous nature of renewable energy resources, robustness of the controller against PnP functionality of DGs is one of the most important requirements of the control system. To that end, in this scenario we analyze the efficiency of the controller concerning the PnP operation of DGs. To perform this scenario, DGs 6 and 8 are simultaneously plugged-out from the microgrid at $t = 1.5s$. Then at $t = 2s$, they are plugged-back into the system. In this scenario, DGs 1 and 5 that are connected to DG 6, and DGs 7 and 10 that are connected to DG 8 are also affected. To analyze the efficiency of the designed controller, performances of DGs 6 and 8 together with their neighbors as the result of this scenario are presented in Fig. 6 and 7, respectively. Fig. 6(a) illustrates the output voltage of DG 6 and shows that the designed control system provides robust stability and robust performance against the PnP operation with small transient and zero steady-state error following IEEE standards [37]. The control signal of DG 6 and the dynamical behaviors of DG 1 and DG 5 are also illustrated in Fig. 6(b), 6(c), and 6(d), respectively. Similar results can be deduced from the dynamical responses of DG 8 and its neighboring DGs illustrated in Fig. 7. Boundedness of the control signal and robust performance and robust stability of the system concerning PnP functionality of the DGs are proven by these results.

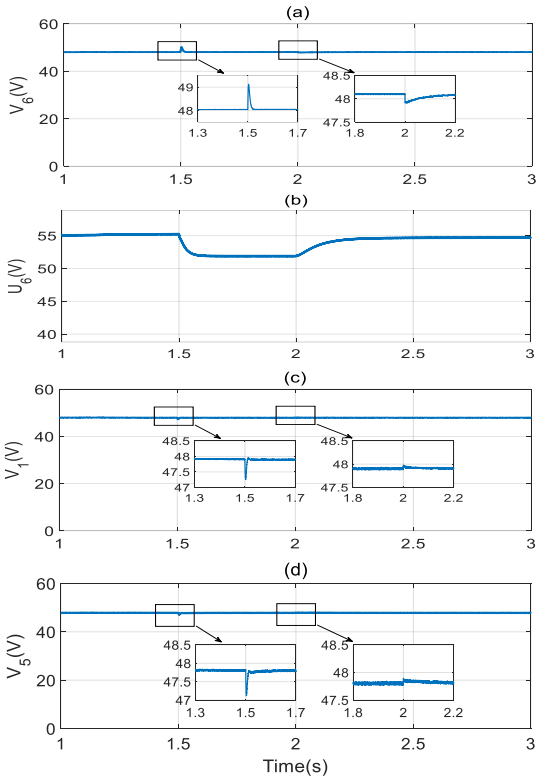

Fig. 6. Performance of the microgrid system concerning PnP functionality of DG 6: (a) dynamical response of DG 6, (b) control signal of DG 6, (c) dynamical response of DG 1, (d) dynamical response of DG 5.

C. Scenario 3: Disconnection of the Distribution Lines

Another objective of the designed control system was providing robust stability and robust performance in case of disconnection of distribution lines. To examine the realization of this objective, the efficiency of the controller concerning this source of uncertainty is analyzed in this scenario. We assume that first at $t = 1s$, the connection between DG 6 and DG 1 and the connection between DG 4 and DG 5 are disconnected, simultaneously. Then at $t = 1.5s$, the connections between DG 2 and DG 1 and DG 5 and 7 are also disconnected. As a result of this topological change, DGs 1, 2, 4, 5, 6, and 7 are affected. The dynamical behaviors of the affected DGs are shown in Fig. 8. It is shown that the disconnection of these distribution lines had a very small transient (under 0.1 seconds) with zero steady-state error on the dynamical responses of these DGs. Therefore, it is proved that the designed control system can maintain the stability and the optimal desired performance of the DC microgrid even in significant changes in the topology of the system with the slightest transient.

D. Scenario 4: Load Variations

In this scenario, we evaluate the performance of the system in tracking voltage references in case of changes in the local loads. For this purpose, load resistance at the PCC of DG 6 is changed from 8 to 4 Ω at $t = 1s$. To evaluate the performance of the designed robust controller with respect to this load change, the PCC voltages of DG 6 and its neighboring DGs

This article has been accepted for publication in a future issue of this journal, but has not been fully edited. Content may change prior to final publication. Citation information: DOI 10.1109/JESTPE.2021.3054723, IEEE Journal of Emerging and Selected Topics in Power Electronics

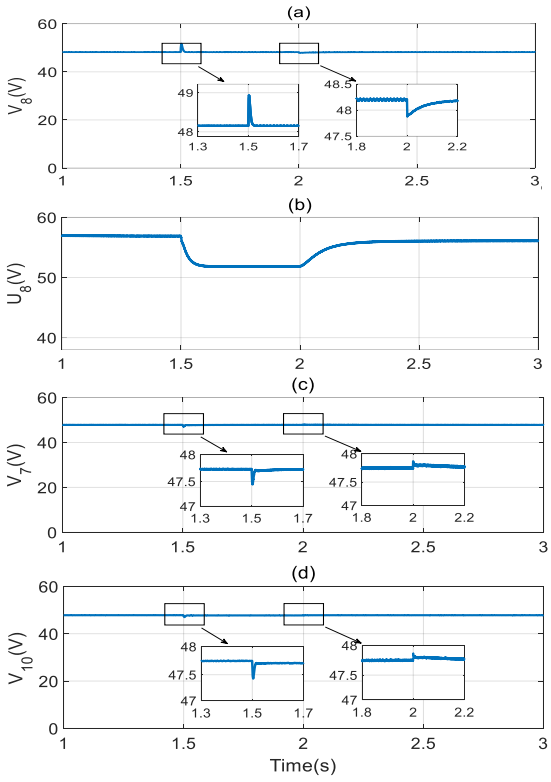

Fig. 7. Performance of the microgrid system concerning PnP functionality of DG 8: (a) dynamical response of DG 8, (b) control signal of DG 8, (c) dynamical response of DG 7, (d) dynamical response of DG 10.

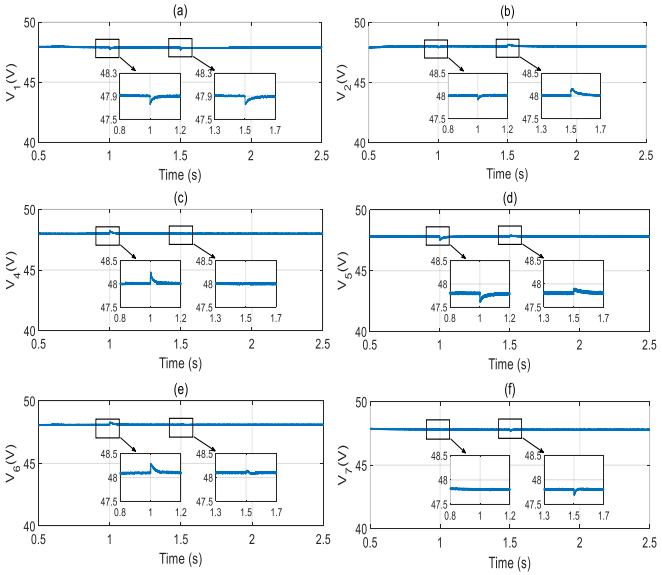

Fig. 8. Performance of the microgrid system concerning disconnection of several distribution lines: (a) dynamical response of DG 1, (b) dynamical response of DG 2, (c) dynamical response of DG 4 (d) dynamical response of DG 5, (e) dynamical response of DG 6, (f) dynamical response of DG 7.

(i.e. DG 1, and 5) are investigated. Fig. 9 shows the results of this study for DG 6 and its neighboring DGs. These results demonstrate that the controller effectively provides robust stability and robust performance with a very small transient

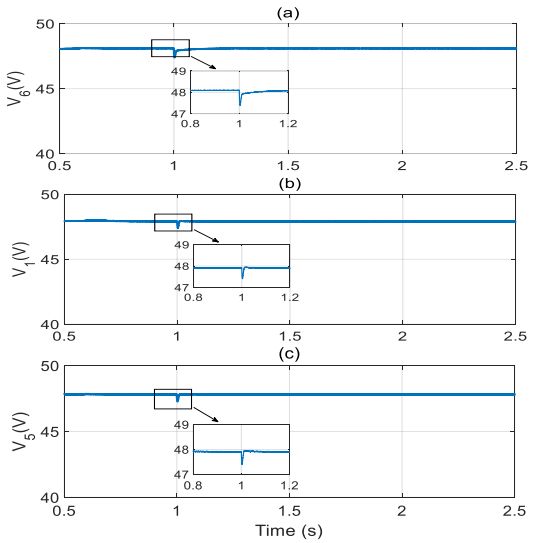

Fig. 9. Performance of the microgrid system concerning load changes: (a) dynamical response of DG 6, (b) dynamical response of DG 1, (c) dynamical response of DG 5.

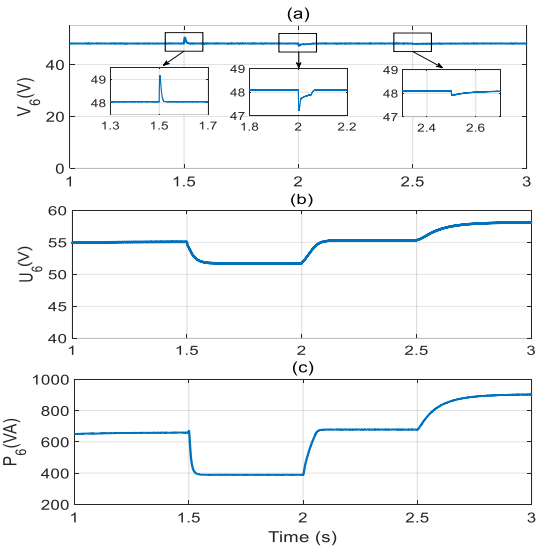

Fig. 10. Dynamic response of the microgrid system against subsequent changes: (a) output voltage at PCC6, (b) control signal of the DG 6, (c) output power at PCC6.

(less than 0.02 seconds) with zero steady-state error for the DC microgrid system under local load changes.

E. Scenario 5: Different Subsequent System Changes

Providing robust stability and robust performance for the DC microgrid when several consecutive changes occur is highly crucial. Unlike previous researches [22]-[27] and due to the robust performance property of the designed control system, the controller provides robustness against different subsequent system changes.

To analyze this property, first DG 6 is plugged-out of the microgrid at $t = 1.5s$. Then, load resistance at the PCC of DG

This article has been accepted for publication in a future issue of this journal, but has not been fully edited. Content may change prior to final publication. Citation information: DOI 10.1109/JESTPE.2021.3054723, IEEE Journal of Emerging and Selected Topics in Power Electronics

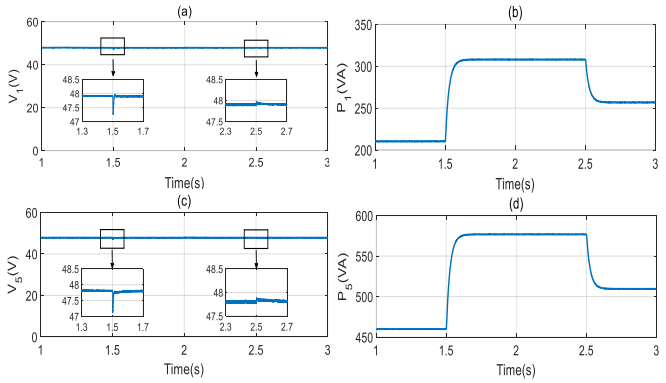

Fig. 11. Dynamic response of the DGs 1 and 5 concerning subsequent changes in DG 6: (a) output voltage at PCC1, (b) output power at PCC1, (c) output voltage at PCC5, (d) output power at PCC5.

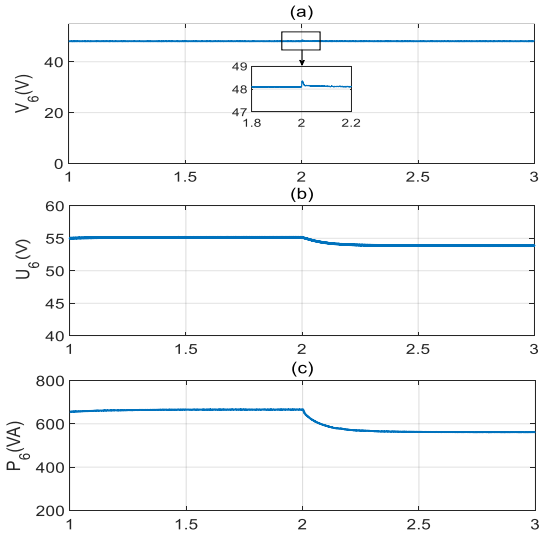

Fig. 12. Performance analysis of the control system against uncertainty in CPLs: (a) output voltage at PCC6, (b) control signal of the DG 6, (c) output power at PCC6.

6 is changed from 8 to 4 Ω at $t = 2s$. Finally, DG 6 is plugged-back into the microgrid at $t = 2.5s$. Fig. 10 illustrates the results of this study for DG 6. The PCC voltage, control signal, and output power of DG 6 are presented in Fig. 10(a), 10(b), and 10(c), respectively. These results indicate the efficiency and robustness of the designed control system in order to maintain the stability and the optimal desired performance of the DC microgrid with small transient and zero steady-state error concerning subsequent changes in the microgrid system.

Also, the effect of these changes on DG 6 neighboring DGs (i.e. DGs 1 and 5) is investigated in Fig. 11. These results show that subsequent changes in DG 6 have a small effect on output voltages of DGs 1 and 5. Therefore, efficiency of the designed robust control system following IEEE standards [37] is proved in case of different subsequent system changes.

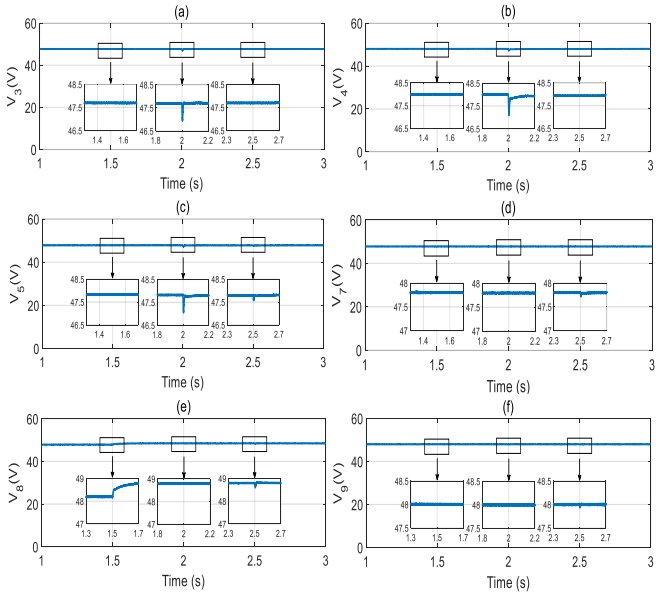

Fig. 13. Performance analysis of the control system for microgrids with radial topology with various changes: (a) output voltage at PCC3, (b) output voltage at PCC4, (c) output voltage at PCC5, (d) output voltage at PCC7, (e) output voltage at PCC8, (f) output voltage at PCC9.

F. Scenario 6: Robustness against Uncertainty in CPLs

In this scenario, we evaluate the effectiveness of the control system against the uncertainty of the CPLs. For this purpose, at $t = 2s$ the power of the CPL inside DG 6 is changed from $120W$ to $180W$. Fig. 12 presents the dynamical response of DG 6 in this regard. The PCC voltage, control signal, and output power of DG 6 are shown in Fig. 12(a), 12(b), and 12(c), respectively. Robust stability and robust desired performance of the closed-loop DC microgrid system with zero steady-state error, slightest transient (less than 0.02 seconds), and Bounded control signal are proven by these results. The results prove the efficiency of the developed robust control system against the uncertainty of CPLs.

G. Scenario 7: Performance Evaluation Under Radial Topology

As mentioned before, the proposed robust control system is designed for a multi-DG microgrid with general topology. Meaning that the designed controller is applicable to DC microgrids with different topologies. Therefore, in this scenario the performance of the control system for microgrids with radial topology under multiple subsequent changes is analyzed.

To achieve a radial topology, DGs 1, 2, and 6 are plugged-out of the system at the beginning of this scenario. It is clear that the remaining DGs form a microgrid with a radial topology. To analyze the performance of the controller in this topology, first at $t = 1.5s$ the reference voltage value of DG 8 is changed from $48.2v$ to $48.8v$. Then, the ohmic load of DG 4 is changed from 2Ω to 6Ω at $t = 2s$. finally, at $t = 2.5s$ the CPL of DG 7 is increased by $30W$. Fig. 13 presents the dynamical responses of all the affected DGs in

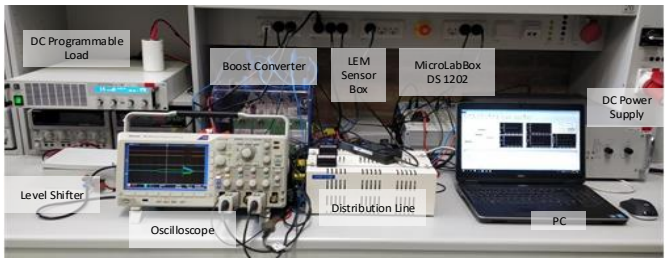

Fig. 14. Experimental setup of a DC microgrid comprising of 2 DG units.

TABLE III
EXPERIMENTAL SETUP PARAMETERS VALUES

DGs Parameters						
DGs	$R_t(\Omega)$	$L_t(mH)$	$C_t(mF)$	$R_L(\Omega)$	$P_{CPL}(W)$	$V_{ref}(V)$
DG 1	0.3	3.0	0.1	10	450	48
DG 2	0.3	3.0	0.1	10	450	48.3

State-Feedback Controller Gains			
DGs	K_1	K_2	K_3
DG1	-0.187	-0.33	42.36
DG2	-0.21	-0.215	38.71

Boosts Input Voltage	$V_{dc} = 36V$
Switching Frequency	$f_{sw} = 10KHz$
Sampling Frequency	$f_s = 20KHz$
Line Parameters Values	$R_{12} = 0.15\Omega$, $L_{12} = 2.5\mu H$

the microgrid in this regard. All these results confirm that the control system effectively regulates the output voltages of all the DGs connected in a radial topology with slightest transient and zero steady-state error following IEEE standards [37].

V. EXPERIMENTAL RESULTS

The proposed voltage control method's performance is validated experimentally using a DC microgrid consisting of 2 DGs with boost converters. The experimental setup is shown in Fig. 14, and Table III presents the parameters values used in the experimental setup. Each DG unit is controlled using only local measurements by dSPACE MicroLabBox DS1202 (target), with control commands from the ControlDesk from the PC (host). The control system's performance is validated using two different scenarios; PnP functionality of DGs and load changes.

The first experiment evaluates the efficiency of the proposed controller against the PnP functionality of DGs. To perform this experimental test, DG1 is plugged-out of the microgrid system at $t = 1.5s$, and then it is plugged-back into the microgrid system at $t = 2.5s$. The PCC voltages of the DGs in the islanded microgrid as the result of this experimental test are presented in Fig. 15(a). The results demonstrate that the designed robust control system provides robust stability and robust performance against PnP operation of DGs with small transient and zero steady-state error following the IEEE standards [37].

The second experiment validates the capability of the proposed control system against local load changes. To carry

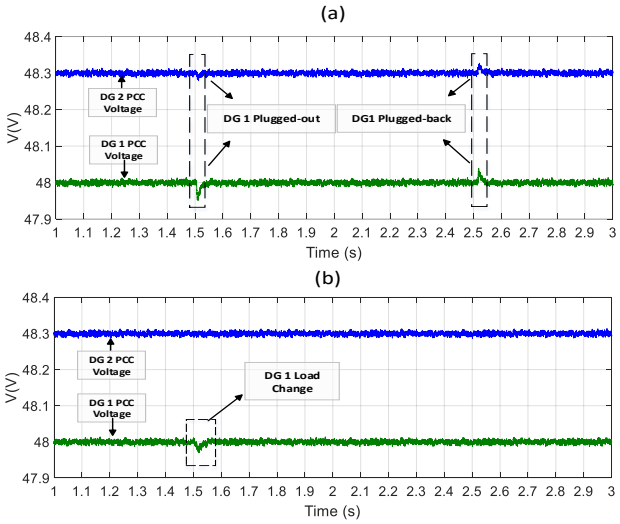

Fig. 15. Experimental validation of the proposed robust voltage control approach for: (a) PnP functionality of DGs, (b) load changes.

out this experiment, the local load of DG 1 is increased by 4Ω at $t = 1.5s$. The PCC voltages of these two DGs resulting from this experimental test are illustrated in Fig. 15(b). The outcomes indicate that the proposed controller effectively provides robust stability and robust performance against local load changes with a very small transient and zero steady-state error following the IEEE standards [37].

VI. CONCLUSION

In this paper, the development of a decentralized optimal one DoF robust H_∞ primary voltage control system for the autonomous DC microgrids is investigated. The presented control system has four distinguishing features compared to the previously designed controllers: 1) The proposed control system not only guarantees robust stability, but it also provides robust performance of the DC microgrid system under multiple sources of uncertainty such as PnP operation of DGs, microgrid topology changes, load variations, subsequent system changes, and presence of the CPLs, 2) The developed one DoF robust controller is the solution of a unique convex optimization problem that results in an optimal controller and an optimal performance, 3) The design of this control system allows us to apply no constraints on Lyapunov matrices to achieve a decentralized strategy, which results in less conservatism, and 4) The robust performance property of the developed controller eliminates the need for any pre-filter design that leads to lower complexity. The developed control system requires no parameter re-tuning after the PnP operation of DGs, and the one DoF design of the control system provides robust stability and optimal robust performance without a need for a secondary controller or any sort of communications. The efficiency and performance of the developed robust control system are confirmed by simulating multiple scenarios, such as voltage reference changing, PnP operation of DGs, disconnection of distribution lines, system topological

This article has been accepted for publication in a future issue of this journal, but has not been fully edited. Content may change prior to final publication. Citation information: DOI 10.1109/JESTPE.2021.3054723, IEEE Journal of Emerging and Selected Topics in Power Electronics

changes, load variations, different subsequent system changes, and uncertainy in the CPLs using SimPowerSystems Toolbox in MATLAB. Moreover, the efficiency of the proposed controller is validated using the experimental testbed.

APPENDIX
PROOF OF THEOREM 1

Proof. We want to prove that the conditions in Theorem 1, will lead to the robust stability and robust H_∞ performance of the overall closed-loop DC microgrid. The convex combination of all of the conditions specified in Theorem 1, results in the following

$$\begin{bmatrix} W_i(\lambda)+\Psi_i(\lambda)+{\Psi_i}^T(\lambda) & * & * & * \\ \zeta_i\Psi_i^T(\lambda)-\bar{A}_{g_{ii}}(\lambda)X_i-\bar{B}_{g_i}Z_i & \Upsilon_i(\lambda) & * & * \\ \bar{B}_{d_i}^T & -\bar{B}_{g_i}^T & -I & * \\ \Gamma_i & \zeta_i\Gamma_i & D_{d_i} & -\gamma I \end{bmatrix} < 0 \tag{30}$$

where

$$\begin{aligned} \Psi_i(\lambda) &= \tilde{A}_{g_{ii}}(\lambda)X_i+\bar{B}_{g_i}Z_i, \quad \Gamma_i = C_{2g_i}X_i+D_{g_i}Z_i \\ \Upsilon_i(\lambda) &= -W_i(\lambda)-\zeta_i\bar{A}_{g_{ii}}(\lambda)X_i-\zeta_i\bar{B}_{g_i}Z_i-\zeta_iX_i^T\bar{A}_{g_{ii}}^T(\lambda) \\ &\quad -\zeta_iZ_i^T\hat{B}_{g_i}^T \\ \tilde{A}_{g_{ii}}(\lambda) &= \epsilon_i\hat{A}_{g_{ii}}(\lambda)-1/2\epsilon_i, \quad \bar{A}_{g_{ii}}(\lambda) = \epsilon_i\hat{A}_{g_{ii}}(\lambda)-1/2\epsilon_i \\ \bar{B}_{g_i} &= \epsilon_i\hat{B}_{g_i}, \quad \bar{B}_{d_i} = \epsilon_i\hat{B}_{d_i} \end{aligned} \tag{31}$$

and $\hat{A}_{g_{ii}}(\lambda)=\sum_{v=1}^{2}\lambda_v\hat{A}_{g_{ii}}^v$, $W_i(\lambda)=\sum_{v=1}^{2}\lambda_vW_i^v$, and X_i has the structure specified in (20).

Defining $\hat{A}_D(\lambda) = diag(\hat{A}_{g_{11}}(\lambda),\ldots,\hat{A}_{g_{NN}}(\lambda))$, $\hat{A}_C = \hat{A}(\lambda)-\hat{A}_D(\lambda)$, $W(\lambda) = diag(W_1(\lambda),\ldots,W_N(\lambda))$, $X = diag(X_1,\ldots,X_N)$, $Z = diag(Z_1,\ldots,Z_N)$, and $z = diag(z_1,\ldots,z_N)$, and based on the Schur's complement lemma in [30], the set of aforementioned conditions for $i=1,\ldots,N$ is

$$\begin{bmatrix} W(\lambda)+\Psi+\Psi^T & * & * & * \\ \zeta\Psi^T-\bar{A}_D(\lambda)X-\bar{B}_gZ & \Upsilon & * & * \\ \bar{B}_d^T & -\bar{B}_g^T & -I & * \\ \Gamma & \zeta\Gamma & D_d & -\gamma I \end{bmatrix} < 0 \tag{32}$$

where

$$\begin{aligned} \Psi(\lambda) &= \tilde{A}_D(\lambda)X+\bar{B}_gZ, \quad \Gamma = C_{2g}X+D_gZ \\ \Upsilon(\lambda) &= -W(\lambda)-\zeta\bar{A}_D(\lambda)X-\zeta\bar{B}_gZ-\zeta X^T\bar{A}_D^T(\lambda) \\ &\quad -\zeta Z^T\hat{B}_g^T \\ \tilde{A}_D(\lambda) &= \epsilon\hat{A}_g(\lambda)-1/2\epsilon, \quad \bar{A}_D(\lambda) = \epsilon\hat{A}_D(\lambda)-1/2\epsilon \\ \bar{B}_g &= \epsilon\hat{B}_g, \quad \bar{B}_d = \epsilon\hat{B}_d \end{aligned} \tag{33}$$

Now by choosing a very small value for η_i in (20), the interaction terms $\hat{A}_{g_{ij}}X_i$ are negligible, because

$$\hat{A}_{g_{ij}}X_i = {X_i}^T\hat{A}_{g_{ij}}^T = \begin{bmatrix} \frac{\eta_i}{R_{ij}C_i} & 0 & 0 \\ 0 & 0 & 0 \\ 0 & 0 & 0 \end{bmatrix} \approx 0 \tag{34}$$
$$i=1,\ldots,N \ \ and \ \ j\in N_i$$

Therefore, term $\hat{A}_CX = X^T\hat{A}_C^T \simeq 0$ and $\hat{A}_D(\lambda)=\hat{A}(\lambda)$. Consequently, the following condition holds and it guarantees the robust stability and robust H_∞ performance of the overall closed-loop DC microgrid [31].

$$\begin{bmatrix} W(\lambda)+\Psi(\lambda)+\Psi^T(\lambda) & * & * & * \\ \zeta\Psi^T-\bar{A}(\lambda)X-\bar{B}_gZ & \Upsilon & * & * \\ \bar{B}_d^T & -\bar{B}_g^T & -I & * \\ \Gamma & \zeta\Gamma & D_d & -\gamma I \end{bmatrix} < 0 \tag{35}$$

where

$$\begin{aligned} \Psi(\lambda) &= \tilde{A}(\lambda)X+\bar{B}_gZ, \quad \Gamma = C_{2g}X+D_gZ \\ \Upsilon(\lambda) &= -W(\lambda)-\zeta\bar{A}(\lambda)X-\zeta\bar{B}_gZ-\zeta X^T\bar{A}^T(\lambda) \\ &\quad -\zeta Z^T\hat{B}_g^T \\ \tilde{A}(\lambda) &= \epsilon\hat{A}(\lambda)-1/2\epsilon, \quad \bar{A}(\lambda) = \epsilon\hat{A}(\lambda)-1/2\epsilon_i \\ \bar{B}_g &= \epsilon\hat{B}_g, \quad \bar{B}_d = \epsilon\hat{B}_d \end{aligned} \tag{36}$$

□

REFERENCES

[1] A. T. Elsayed, A. A. Mohamed, and Q. A. Mohamed, "DC microgrids and distribution systems," *Electric Power Systems Research*, vol. 119, no. 4, pp. 407-417, Feb. 2015.

[2] M. E. Baran, and N. R. Mahajan, "DC microgrids and distribution systems:opportunities and challenges," *IEEE Trans. Industry Applications,* vol. 39, no. 3, pp. 1596-1601, Nov. 2003.

[3] D. Salomonsson, and A. Sannino, "Low-voltage DC distribution system for commercial power system with sensitive electronic loads," *IEEE Trans. Power Delivery,* vol. 22, no. 3, pp. 1620-1627, July. 2007.

[4] D. Boroyevich, I. Cvetkovic, D. Dong, R. Burgos, W. Fei, and F. Lee, "Future electronic power distribution systems: a contemplative view," *in 12th International Conference on Optimization of Electrical and Electronic Equipment (OPTIM)*, May 2010, pp. 1369-1380.

[5] D. E. Olivares, A. Mehrizi-Sani, A. H. Etemadi, C. A. Canizares, R. Iravani, M. Kazerani, A. H. Hajimiragha, O. Gomis-Bellmunt, M. Saeedifard, R. Palma-Benke, G. A. Jimenez-Bellmunt, and N. D. Hatziargyrios, "Trends in microgrid control", *IEEE Trans. Smart Grid,* vol. 5, no. 4, pp. 1905-1919, May. 2014.

[6] J. M. Guerrero, M. Chandorkar, T. Lee, and P. C. Loh, "Advanced control architectures for intelligent microgrids-Part I: Decentralized and hierarchical control", *IEEE Trans. Ind. Electron.,* vol. 60, no. 4, pp. 1254-1262, Apr. 2013.

[7] L. Meng, Q. Shafiee, G. Ferrari Trecate, H. Karimi, D. Fulwani, X. Lu, and J. M. Guerrero, "Review on Control of DC Microgrid and Mutiple Microgrid Clusters," *IEEE Journal of Emerging and Selected Topics in Power Electronics,* vol. 5, no. 3, pp. 928-948, Mar. 2017.

[8] C. Dong, and X. Lie, "Autonomous DC Voltage Control of a DC Microgrid with Multiple Slack Terminals," *IEEE Trans. Power Systems* vol. 27, no. 4, pp. 1897-1905, Apr. 2012.

[9] S. Anand, and B. G. Fernandes and M. Guerrero, "Distributed control to ensure proportional load sharing and improve voltage regulation in low-voltage DC microgrids," *IEEE Trans. Power Electron.,* vol. 28, no. 4, pp. 1900-1913, Apr. 2013.

[10] P. H. Huang, P. C. Liu, W. Xiao, and M. S. El Moursi, "A Novel Droop-Based Average Voltage Sharing Control Strategy for DC Microgrids," *IEEE Trans. Smart Grid,* vol. 6, no. 3, pp. 1096-1106, Sep. 2015.

[11] A. Khorsandi, M. Ashourloo, and H. Mokhtari, "A Decentralized Control Method for a Low-Voltage DC Microgrid," *IEEE Trans. Energy Conversion,* vol. 29, no. 4, pp. 793-801, Jun. 2014.

[12] J. M. Guerrero, J. C. Vasquez, J. Matas, L. G. de Vicuna, and M. Castilla, "Hierarchical control of droop-controlled AC and DC microgrids-A general approach towards standardization," *IEEE Trans. Ind. Electron.,* vol. 58, no. 1, pp. 158-172, Jan. 2011.

[13] X. Lu, M. Guerrero, K. Sun, and J. C. Vasquez, "An improved droop control method for DC microgrids based on low bandwidth communication with DC bus voltage restoration and enhanced current sharing accuracy," *IEEE Trans. Power Electron.,* vol. 29, no. 4, pp. 1800-1812, Apr. 2014.

[14] L. Meng, T. Dragicevic, J. M. Guerrero, and J. C. Vasquez, "Dynamic consensus algorithm based distributed global efficiency optimizayion of a droop controlled DC microgrid," *IEEE Energy Conference (ENERGYCON14)*, Cavtat, Croatia, May 2014, pp. 1276-1283.

[15] A. H. Etemadi, E. J. Davison, and R. Iravani, "decentralized robust control strategy for multi-DER microgrids—Part I: Fundamental concepts," *IEEE Trans. Power Del.,* vol. 27, no. 4, pp. 1843-1853, Oct. 2012.

[16] M. S. Sadabadi, Q. Shafiee, and A. Karimi, "Plug-and-play voltage stabilization in inverter-interfaced microgrids via a robust control strategy," *IEEE Trans. Control Syst. Technol.,* vol. 25, no. 3, pp. 781-791, Apr. 2017.

[17] S. Riverso, F. Sarzo, and G. Ferrari-Trecate, "Plug-and-play voltage and frequency control of islanded microgrids with meshed topology," *IEEE Trans. Smart Grid,* vol. 6, no. 3, pp. 1176-1184, May. 2014.

[18] M. S. Sadabadi, A. Haddadi, H. Karimi, and A. Karimi, "A robust active damping control strategy for an LCL-based grid-connected DG unit," *IEEE Trans. Ind. Electron.,* vol. 64, no. 10, pp. 8055-5065, Apr. 2017.

[19] A. H. Etemadi, E. J. Davison, and R. Iravani, "A generalized decentralized robust control of islanded microgrids," *IEEE Trans. Power Syst.,* vol. 29, no. 6, pp. 3102-3113, Nov. 2014.

[20] M. Babazadeh, and H. Karimi, "A robust two-degree-of-freedom control strategy for an islanded microgrid," *IEEE Trans. Power Del.,* vol. 28, no. 3, pp. 1339–1347, Jul. 2013.

[21] S. Derakhshan, M. Shafiee-Rad, Q. Shafiee, and M. R. Jahed-Motlagh, "Decentralized Robust Voltage Control of Islanded AC Microgrids: An LMI-Based H_∞ Approach," *11th Power Electronics, Drive Systems, and Technologies Conference (PEDSTC),* pp. 1-6, Feb. 2020.

[22] M. Mehdi, M. Saad, S. Z. Jamali, and Kim CH "Output-feedback based robust controller for uncertain DC islanded microgrid," *IEEE Trans. Institute of Measurement and Control,* vol. 42, no. 6, pp. 1239-1251, Apr. 2020.

[23] M. Mehdi, S. Z. Jamali, M. O. Khan, S. Baloch, and C. H. Kim "Robust control of a DC microgrid under parametric uncertainty and disturbances," *Electric Power Systems Research,* vol. 179, no. 1, pp. 106074, Feb. 2020.

[24] M. s. Sadabadi, and Q. Shafiee, "Scalable Robust Voltage Control of DC Microgrids with Uncertain Constant Power Loads," *IEEE Trans. Power Syst.,* Jul. 2019.

[25] M. Tucci, S. Riverso, J. C. Vasquez, J. M. Guerrero, and G. Ferrari-Trecate, "A decentralized scalable approach to voltage control of DC islanded microgrids," *IEEE Trans. Control Syst. Technol.,* vol. 24, no. 6, pp. 1965-1979, Nov. 2016.

[26] M. Tucci, S. Riverso, and G. Ferrari-Trecate, "Line-independent plug-and-play controllers for voltage stabilization in dc microgrids," *IEEE Trans. Control Syst. Technol.,* vol. 26, no. 3, pp. 1115-1123, May. 2017.

[27] M. s. Sadabadi, Q. Shafiee, and A. Karimi, "Plug-and-play robust voltage control of DC microgrids," *IEEE Trans. Smart Grid,* vol. 19, no. 6, pp. 6886-6896, Nov. 2017.

[28] J. Mahdavi, A. Etemadi, and H. A. Toliyat, "Application of state space averaging method to sliding mode control of PWM DC/DC converters," *IEEE Industry Applications Society Annual Meeting,* New Orleans, Louisiana, Oct. 1997.

[29] V. Venkatasubramanian, H. Schattler, and J. Zaborszky, "Fast time varying phasor analysis in the balanced three-phase large electric power system," *IEEE Trans. Automat. Control,* vol. 40, no. 11, pp. 1975-1982, Nov. 1995.

[30] K. Zhou and J. C. Doyle, Essentials of robust control, N. Y.: Prentice-Hall, 1998.

[31] L. A. Rodrigues, E. C. L. F. Oliveira, and J. F. Camino, "Parametrized LMIs for robust and state feedback control of continous-time polytopic systems," *International Journal of Robust and Nonlinear Control,* vol. 28, no. 3, pp. 940-952, Feb. 2018.

[32] A. Emadi, A. Khaligh, C. H. Rivetta, and G. A. Williamson, "Constant power loads and negative impedance instability in automotive sustems: Definition, Modeling, stability, and control of power electronic converters and motor drives," *IEEE Trans. Veh. Technol.,* vol. 55, no. 4, pp. 1112-1125, Jul. 2006.

[33] J. Löfberg,"YALMIP: A toolbox for modeling and optimization in MATLAB," *in proc. IEEE Int. Symp. Comput. Cont. Syst. Design (CACSD),* pp. 284-289, Sep. 2004.

[34] J. F. Strum,"Using SeDuMi 1.02, A Matlab toolbox for optimization over symmetric cones," *Optimization Methods and Software,* vol. 11, no. 1-4, pp. 625-653, Jan. 1999.

[35] S. Buso and P. Mattavelli, "Digital control in power electronics," *Lectures on power electronics.,* vol. 1, no. 1, pp. 1-158, Jan. 2006.

[36] H. Tu, Y. Du, H.Yu, A. Dubey, S. Lukic, and G. Karsai, "information architecture platform for the smart grid (riaps): a novel open-source platform for microgrid control," *IEEE Trans. Ind. Electron.,* Nov. 2019.

[37] "IEEE recommended practice for monitoring electric power quality, IEEE standard1159,"2019.